Social Reactivation of Fear Engrams Enhances Memory Recall

Authors: Abby Basya Finkelstein[1,2*], Héloïse Leblanc[1,3†], Rebecca H. Cole[1†], Troy Gallerani[1,3], Anahita Vieira[1,4], Yosif Zaki[1,5], Steve Ramirez[1*]

Affiliations

[1]Department of Psychological and Brain Sciences, Boston University, Boston, MA, USA.

[2]Department of Molecular and Cellular Biology, Harvard University, Cambridge, MA, USA.

[3]Boston University School of Medicine, Boston, MA.

[4]The Broad Institute of MIT and Harvard, Cambridge, MA, USA.

[5]Icahn School of Medicine at Mount Sinai, NYC, NY, USA.

[†]Co-second Authors

* Correspondence to: afinkelstein@fas.harvard.edu and dvsteve@bu.edu

Summary

For group-living species such as humans and rodents, conspecific interactions pervasively shape emotion [3–5], attention [6], and cognitive ability [7–10]. Higher-order cognitive processes such as memory within a social brain are thus interlaced with social influences. Traditional laboratory rodent cages offer a limited but nonetheless rich multi-modal landscape of communication, including auditory calls [11–14], chemical signaling [15,16], and tactile stimulation [17,18]. The absence of such social encounters in singly housed animals results in cognitive impairments and depression-like phenotypes [23], likely obscuring how the social brain has evolved to function. It is thus important to understand the relationship between social context and how individuals process memories. As social interaction recruits hippocampal [29] and amygdalar [30] circuitry that also serves as hubs for non-social memory traces[24–28], we hypothesized that pre-existing ensembles in these regions can be modulated by social experiences and lead to changes in memory expression. Here we show that stressful social experiences enhance the recall of previously acquired fear memories in male but not female mice. Activity-dependent tagging of cells in the dentate gyrus (DG) during fear learning revealed that these ensembles were endogenously reactivated during the social experiences in males. These reactivated cells were shown to be functional components of

engrams, as optogenetic stimulation of the cells active during the social experience in previously fear conditioned animals was sufficient to drive fear-related behaviors. Our findings suggest that social encounters can reactivate pre-existing DG engrams and thereby strengthen discrete memories.

Keywords: social, memory, recall, c-FOS, engram, dentate gyrus

Results and Discussion

Post-learning social stress amplifies behavioral expression of fear recall in a sex-dependent manner

To assess how social experiences influence existing memories, male and female mice were subjected to social or non-social salient events in the day between contextual fear conditioning (FC) and memory recall tests (**Fig. 1A**). A socially salient experience was provided in various forms: interaction with an unfamiliar juvenile intruder placed in the subject's homecage [31,32] to create a salient and mildly stressful event (Juvenile Intruder group); interaction with a recently shocked cagemate in the homecage to simulate a stressed familiar conspecific (Full Interaction group); indirect non-visual and non-physical exposure to a recently shocked cagemate in the homecage behind a 1-way mirror that permits unidirectional visual access for the shocked mouse to see the cagemates on the other side to simulate ambient exposure to conspecifics' stress (1-Way Mirror group, **Fig. S1**); exposure to a recently shocked cagemate in the homecage through the same mirror covered in opaque black material to block both sides' visual access (Opaque group). A non-social, salient experience was provided in the form of individual restraint stress in a tube (Restraint group), while a social but non-stressful experience was provided via interaction with a cagemate in the homecage (Cagemate control) or with a female mouse (Female Exposure) (**S Methods**). Additional control groups included mice that did not experience any events in the day between FC and recall (Neutral group), and mice that were exposed solely to the novel

50 objects presented in the experimental groups without the associated salient events: the 1-way mirror object (Mirror No Mouse group) and the restraint tubes (Tubes group) to determine the impact of the novelty component (**S Methods**).

Males exhibited higher levels of baseline freezing and froze more than females after the first two shocks of fear conditioning, after which freezing levels were similar (**Fig. S2B**), corroborating tone-cued 55 experiments that report higher levels of freezing in males during acquisition [33]. For males, all control groups exhibited similar freezing during recall and generalization tests to the Neutral group (**Fig. S2C and D**), indicating that the novel objects, as well as the non-stressful social experiences, did not impact recall. The Restraint group also performed similarly during recall and generalization tests to the Neutral group, suggesting that direct physical stress does not alter a previously established fear memory. Both 60 the Juvenile Intruder and 1-Way Mirror groups froze more than the Neutral group during the recall test (**Fig. 1B**), despite similar levels of generalization (**Fig. 1C**), indicating that specifically social events enhance recall. Recent work has shown that observing a conspecific experience the unconditioned stimulus (US) of electric shock results in the reinstatement of context-specific fear[28]; our data suggests the possibility that it is the conspecific's general stressed state rather than a specific response to the US 65 that amplifies the observer's fear memory.

We found that there was a subsequent enhancement of recall only if the stressed cagemate could see the experimental mice through a 1-way mirror; the Opaque group (in which a wall obscured the stressed cagemate's visual access) froze the same as the Neutral group during recall, but exhibited higher difference scores, suggesting reduced generalization (**Fig. 1C**). The blocking of enhanced recall 70 when the stressed cagemate can not see the other mice suggests the intriguing possibility that distressed mice emit different auditory-olfactory stimuli based on their perceived social context.

The Full Interaction group also froze the same as the Neutral group during recall, indicating that direct interaction between the experimental mice and stressed cagemate blocked the effect on recall. Although counterintuitive at first, it is crucial to note that physical interaction with a stressed familiar cagemate is not simply a heightened version of either the passive exposure to stressful emissions or of the interaction with an unfamiliar juvenile intruder mouse. We propose two possibilities for why the memory enhancement is blocked when mice are permitted to fully engage with the stressed familiar cagemate: social buffering [2,34,35]; in which the experimental mice reduce the shocked cagemate's distress, and interference [36–38] in which the intensity of physical contact with the shocked cagemate leads to the formation of a new social memory that interferes with the strengthening of the old fear memory in the experimental mice.

Females, on the other hand, exhibited no effect of either social or non-social experience on freezing during recall (**Fig. 1D**). The only difference in memory occurred for generalization of fear; both Mirror No Mouse and Tube Control groups exhibited elevated difference scores compared to the Neutral group (**Fig. S2F**), indicating that when presented in the absence of other salient experience, novel object exposure following fear conditioning can reduce the generalization of fear in females.

These results demonstrate that intervening experiences between fear conditioning and recall can impact the intensity and context-specificity of fear expression in a sex-dependent manner. Socially salient experiences, but not physical stressors, can enhance fear recall in males but not females.

Socially salient events reactivate ensembles previously active during fear conditioning

To test the hypothesis that fear memories are reactivated in the DG during the social experience for males and not for females, we used a cFos-based activity-dependent viral strategy (**Fig. 2A**) to track fear ensembles processed in the DG and BLA post-fear conditioning **(**representative images, **Fig. 3B**).

95 As predicted, females did not exhibit reactivation of the DG fear trace during the social experience (**Fig. 2F**), while males exhibited reactivation during both the 1-Way Mirror and Juvenile Intruder social experiences (**Fig. 2D**). For males, Juvenile Intruder groups had more active cells, as identified by cFos expression, than 1-Way Mirror groups in both the DG and BLA (**Fig. 2D**). The increased level of DG activity during exposure to a juvenile intruder compared to a stressed cagemate behind a 1-way mirror,
100 (**Fig. 3D**) despite both experiences occurring in the animal's homecage, highlights the DG's role in encoding experiences beyond physical contexts per se [39]. We posit that the higher level of activity in the BLA and DG during exposure to a juvenile intruder reflects the richness of direct social interaction during the juvenile intruder's presence that is not permitted in the 1-way mirror paradigm.

Neither sex demonstrated DG fear trace reactivation during the non-social stressors of restraint
105 or immediate shock (**Fig. 2D, left**), and previous work shows that fear trace reactivation does not occur in neutral contexts [40], supporting the socially-specific nature of this reactivation. Conversely, in the BLA, both Juvenile Intruder and Restraint groups displayed reactivation of tagged cells in males (**Fig. 2D, right**), suggesting that the common denominator of direct physical stress in the form of restraint or interaction with an intruder might recruit amygdalar ensembles also activated during fear conditioning
110 the previous day.

To test whether the reactivation of the fear trace in males occurred only during events happening directly after fear conditioning, we also tracked reactivation of the fear memory following a two day extinction protocol (**Fig. 3A,** representative images in **3b**), after which mice froze significantly less in the fear context (**Fig. 3C**). The percentage of cFos+ cells in DG was slightly but consistently higher
115 during non-social restraint stress than during the social experience (**Fig. 3D, left**), indicating a higher level of overall DG activity. Similar to pre-extinction, the DG fear ensemble was reactivated during the social experience but not during non-social restraint, and the BLA fear ensemble was reactivated during

non-social restraint (**Fig. 3E**). Unlike our pre-extinction results, post-extinction the BLA fear ensemble was also reactivated during the 1-Way Mirror experience (**Fig. 3E**). It is important to note that our data indicate that a significant portion of the fear ensemble was reactivated and may not reflect whether the reactivated subset of cells are the same or different across these experiences.

Collectively these data suggest that specifically social situations reactivate subsets of fear ensembles in the DG for males and not females, and do so even after extinction training. Strikingly, the degree of DG cellular reactivation during the social encounter in males both before and after extinction was similar to previously reported results in animals re-exposed to the original fear context [41]. These results are consistent with the theory that endogenous reactivation of fear ensembles enhances recall [42] and is the mechanism by which multiple exposures to the contexts [43] or cues [44] present during conditioning can strengthen memories in the days after learning. We show that this reactivation does not occur during non-social physical stress, and previous work has shown that it does not occur in neutral contexts [40], supporting the idea of a causal relationship between reactivation and enhanced recall. Given the malleability of engrams [45,46], the natural reactivation of a fear memory ensemble during a stressful social experience could plausibly add additional negative valence from the current experience to the representation of the former, explaining why a single negative social encounter enhances fear whereas multiple exposures to associated neutral contexts [43] are necessary for enhancement.

Stressful social situations activate fear-driving DG ensembles in previously fear conditioned mice

Next, we aimed to investigate the functional properties of the cells which were active during exposure to a stressed cagemate in previously fear-conditioned animals. Fear ensemble reactivation in the DG was correlated specifically with the social experiences that heightened recall, while reactivation in the BLA was more variable. Thus, we hypothesized that the fear ensembles reactivated in the DG were comprised

of fear-activating cells while the ensembles reactivated in the BLA were comprised of non fear-driving components of the ensemble. We predicted that the fear ensembles reactivated during social stress in the DG, but not in the BLA, would cause the cells tagged during this period to drive fear behaviors when optogenetically stimulated. To this end, we tagged DG or BLA cells with channelrhodopsin-2 during our 1-way mirror paradigm or during a neutral home-cage period (**Fig. 4a-d;** See Methods). To ensure that we were not capturing a persistent fearful state but rather the re-emergence of a fear ensemble, we chose to first employ a two day extinction protocol before tagging the cells active during the social or neutral experience. As we show in Figure 3, this timing still results in reactivation of the fear conditioning ensemble. The following day, the tagged ensembles were stimulated in a novel context to test their capacity to drive fearful behavior.

In support of our hypothesis, 20Hz stimulation of the DG ensembles active during the social experience in previously fear conditioned animals drove higher levels of freezing during the light-on sessions (**Fig. 4J**) as well as increased self-grooming (**Fig. 4K**) in the light-off period following stimulation, which is thought to reflect a de-arousing behavioral state[47]. To ensure that this effect was not due simply to negatively valenced cells active during social stress or active post-FC regardless of social experience, we showed that fear behaviors were not induced by either stimulation of cells active in a social setting without prior fear conditioning, or of cells active in a neutral setting after fear conditioning (**Fig. 4, 4K**). The size of the labeled ensembles did not differ between any of these three groups (**Fig. S3E**), indicating that DG activity levels were generally similar and it was not the number of tagged cells but their functionality as fear driving cells that induced fear. In the context of the social experience, the functional capacity of the active ensembles in the DG to drive obvious fear behaviors was quiescent (example **Movie S1** and **Movie S2**), however, we postulate that the more nuanced

documented deficits in social interaction following trauma [50–53] could in part be driven by DG fear ensemble activation.

The coactivation of ensembles leads to co-allocation and the linking of memories, as shown in both mouse [48] and human [49] studies. Our data suggests that during salient social experiences, the DG is concurrently reactivating a pre-existing fear engram and processing the current social stimuli (**Fig. 2**). We therefore posit that the reactivated subset of the fear ensemble was co-allocated to form part of the ensemble encoding the social encounter, perhaps explaining why the total number of cells active during the social exposure was similar regardless of prior fear conditioning (**Fig. 4I**) and why stimulation drove fearful behaviors only in the previously fear conditioned animals (**Fig. 4J and 4K**).

On the other hand, the number of tagged cells in the BLA was higher during social stress if mice had been previously fear conditioned **(Fig. S3F**), suggesting that the combination of prior fear conditioning and social stress leads to heightened amygdalar activity. This is consistent with the notion that sustained amygdalar hyperactivity underlies persistent potentiation of fear and anxiety after stressful events [54]; in rats, prior stress reduces inhibitory control in the BLA, increasing excitability and plasticity [55]. Counterbalanced 20Hz and 4Hz stimulation of cells tagged during social stress did not cause freezing or grooming (**Fig. 4H**), indicating that the amygdalar cells that were active during both FC and social stress (**Fig. 3E**) did not comprise the portion of the original fear engram that drives freezing.

Collectively, these results indicate that the DG ensemble activated during exposure to a stressed cagemate includes a previously established functional fear engram, while the active BLA ensemble is not composed of fear-driving cells.

Conclusion

185 Memory recall is a malleable phenomenon that can be altered by intervening experiences, as associated context or cues can reactivate engrams and thus make them labile during incubation [42–44,56]. In this study, we discovered that even in the absence of associated reminders, salient social encounters can strengthen a pre-existing fear memory in males, but not in females. We explored the role of endogenous cellular reactivation of fear conditioning ensembles in the hippocampus and amygdala during
190 subsequent social vs non-social salient events. While the two forms of socially salient events induced reactivation of the fear ensemble in the DG, the two forms of non-social physical stress did not cause reactivation. Unlike in the DG, reactivation in the BLA was not associated with the social, memory-enhancing experiences. To determine the functional nature of the ensembles activated during the social experiences, we optogenetically tagged these cells and artificially stimulated them with light in neutral
195 conditions. We found that light-induced stimulation caused fear behaviors only when mice had been previously fear conditioned and when the cells stimulated were tagged during the social experience, suggesting that the ensembles reactivated by socially salient events are fear-driving engrams. Thus, we propose that DG engram reactivation provides a mechanism for stressful social experience to potentiate negative memories. Future studies are necessary to confirm the causal role of engram reactivation with
200 an activation-blocking strategy such as chemogenetics while avoiding potentially confounding compensatory effects[51, 52].

For both humans and mice, healthy social conditions include not only positive but also moderately stressful interactions. While extreme social stress can impair memory capabilities [10], a rich social life can protect [9] and enhance [7] memory. Although this enriching effect on learning and memory
205 is often discussed as a function of positive social support, our findings suggest that mildly negative social exposure to conspecifics' stress also plays an important role in strengthening pre-existing memory. From an evolutionary perspective, a stressed conspecific or their ambient auditory-olfactory

emissions might signal a dangerous situation in which it is adaptive to hone one's own memories to guide decision making. Altogether, our findings provide evidence that the mnemonic contents of a social animal's brain are modulated throughout the course of social experiences, and we anticipate ensuing studies to unravel the circuitry bridging social sensory inputs and pre-existing hippocampal engrams.

Main Figures

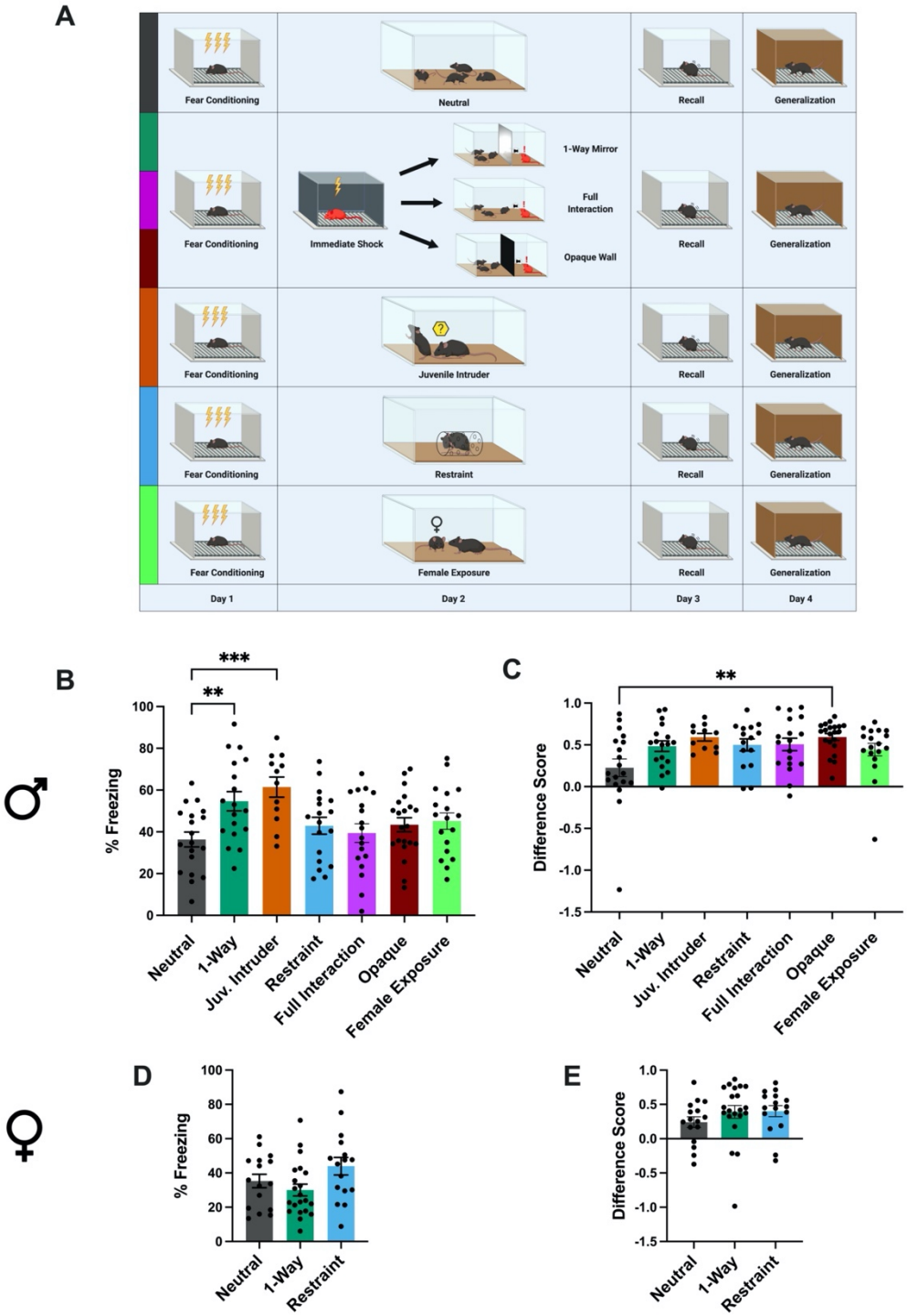

Figure 1. Social stimuli modulate subsequent fear recall in a sex-dependent manner A) Schematic representation of behavioral schedule. **B** and **D**) Freezing levels during a 5 minute fear recall test for

235 males (**B**) and females (**D**). Males: 1-Way ANOVA$F_{(6, 117)}$=3.984, p=0.0012; Holm-Sidak's multiple comparisons: ***p=0.0008 for Neutral vs Juvenile Intruder; **p=0.0082 for Neutral vs 1-Way Mirror. Females: 1-Way ANOVA$F_{(2, 50)}$=2.921, p=0.0631. **C** and **E**) Differences scores, defined as [(freezing in recall test)-(freezing in generalization test)]/(freezing in recall test) for males (**C**) and females (**D**). Males: Kruskal-Wallis statistic=13.34, p=0.0379; Dunn's multiple comparisons: **p=0.0042 for Neutral

240 vs Opaque. Females: ANOVA$F_{(2, 50)}$=0.9847, p=0.3807). Data shown as mean +/- SEM. See also **Fig S2**.

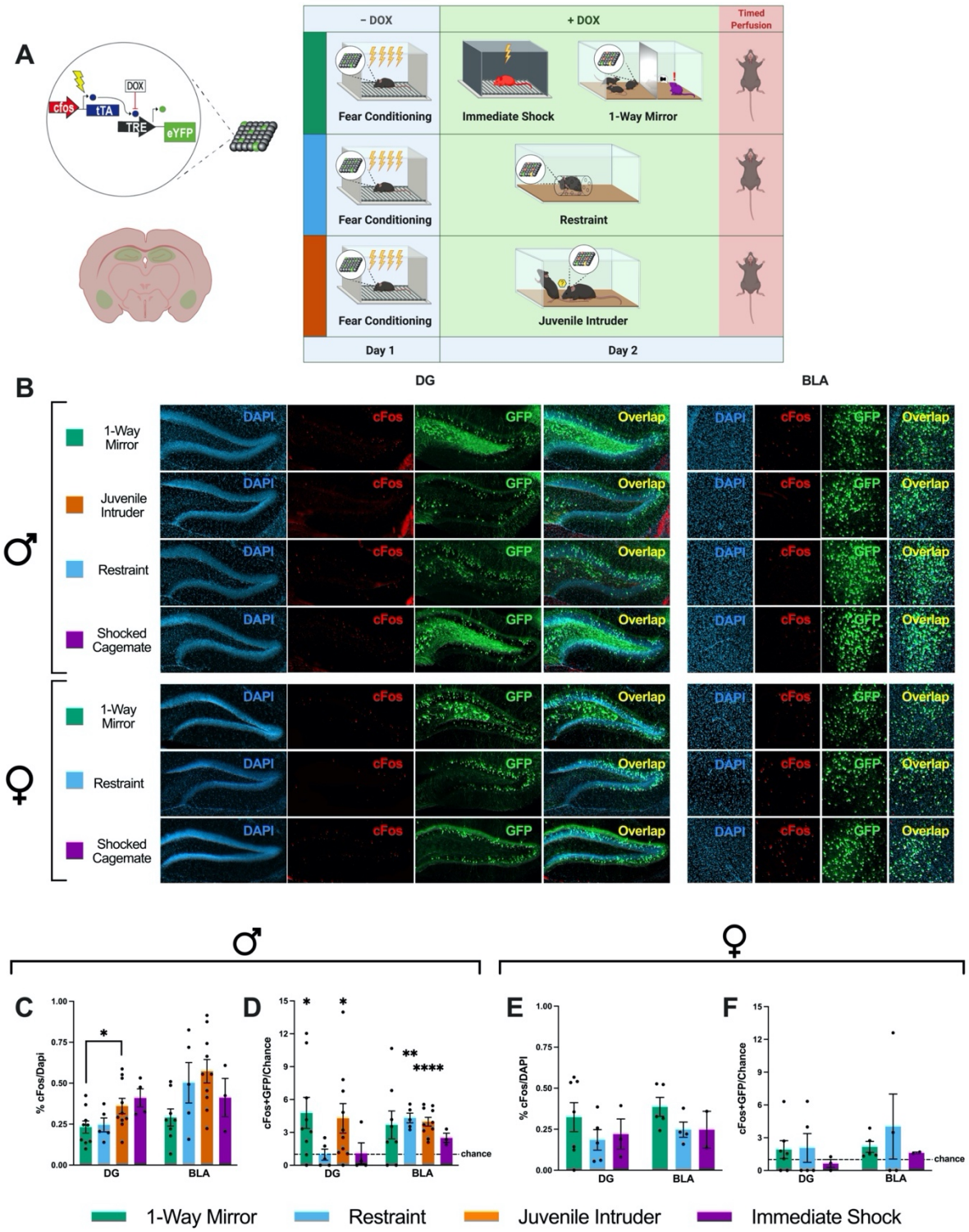

Figure 2. Socially salient but not directly stressful experiences reactivate pre-existing fear ensembles. A) Schematic representation of the doxycycline mediated viral tagging construct (left) and

experimental design (right). **B**) Representative confocal images of DG and BLA histology visualizing cFos-tTa+Tre-EYFP positive cells (active during FC, green) and cFos positive cells (active during the different types of stress exposure, red). **C** and **E**) Percentage of cFos positive cells over DAPI positive cells across brain regions in males and females (Males: DG - 1Way ANOVA$F_{(3, 24)}$=3.028, p=0.0490,
250 Holm-Sidak's multiple comparisons: *p=0.0339 for Juvenile Intruder vs 1-Way Mirror; BLA - 1Way ANOVA$F_{(3, 22)}$=2.710, p=0.0697. Females: DG - 1Way ANOVA$F_{(2, 12)}$=0.4090, p=0.6732; BLA - ANOVA$F_{(2,8)}$=0.3885, p=0.6902). **B** and **D)** Degree of overlap between the two labeled populations normalized over chance (%cFos/DAPI * %EYFP/DAPI). 1-sample t-tests. Males: DG - Juvenile Intruder t=2.436, df=9, *p=0.0376; 1-Way Mirror t=2.656, df=8, *p=0.0290. BLA - Juvenile Intruder
255 t=7.411, df=9, ****p<0.0001; Restraint t=7.462, df=4, 0.0017, **p=0.0017). See details for non-significant results in supplementary text. Data shown as mean +/- SEM. Dotted line represents chance.

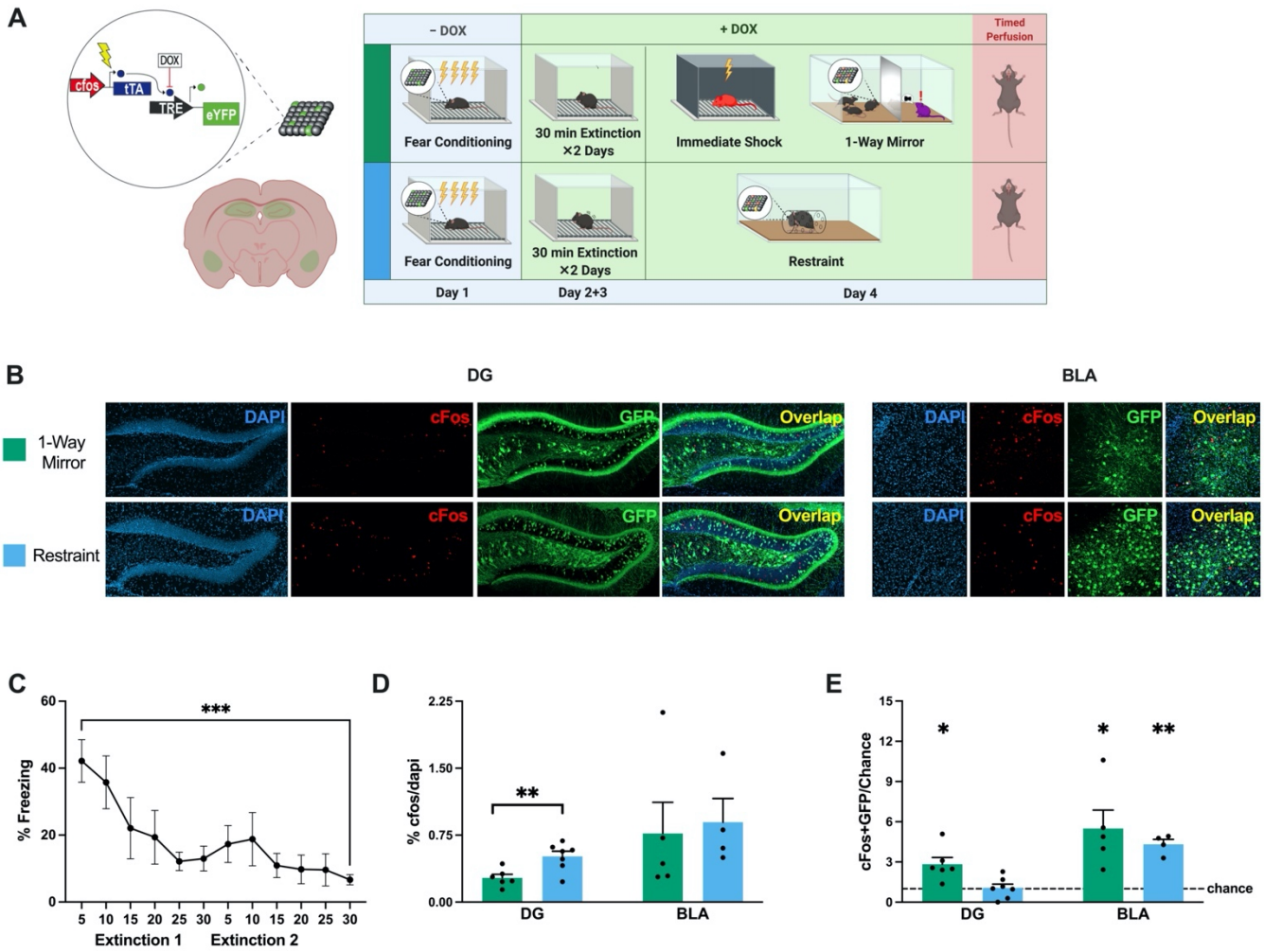

Figure 3. Socially salient experiences reactivates fear ensembles post fear extinction. A) Schematic representation of the doxycycline mediated viral tagging construct (left) and experimental design (right). **B)** Confocal visualization of DG and BLA histology showing cFos-tTa+Tre-EYFP labelled cells (active during FC, green) and cFos+ cells (active during the different types of stress exposure, red). **C)** Freezing throughout extinction training (RM 1Way ANOVA$F_{(3.230,\ 25.84)}$=5.165, p=0.0054, Holm-Sidak's multiple comparisons for first vs last 5 minutes, n=9, t=5.688, ***p=0.0005). **D)** Percentage of cFos+ cells per DAPI+ cells (DG - t-test, t=3.268, df=11, **p=0.0075; BLA - t-test, t=0.2716, df=7, p=0.7938). **E)** Degree of overlap between the two labeled populations normalized over chance (%cFos/DAPI *

%EYFP/DAPI). 1-sample t-tests. DG - Restraint t=0.195, df=6, p=0.8516; 1-Way Mirror t=3.67, df=5, *p=0.0153. BLA - Restraint t=9.031, df=3, **p=0.0029; 1-Way Mirror t=3.257, df=4, *p=0.0312). Dashed line represents chance. Data shown as mean +/- SEM.

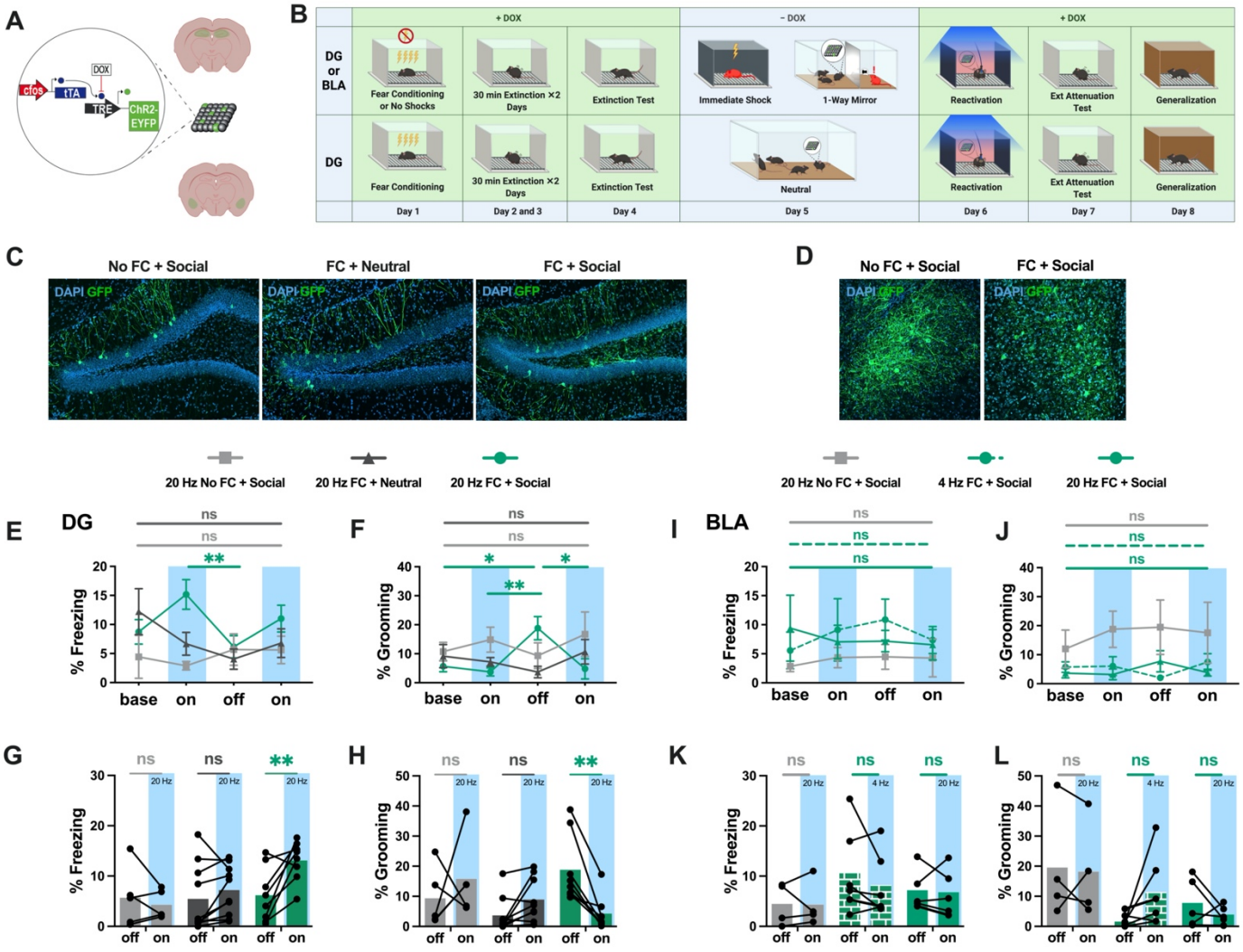

Figure 4. DG ensembles active during social stress drive fear only in previously fear conditioned mice. A) Schematic representation of activity-dependent engram tagging strategy. **B)** Behavioral schedule. **C** and **D)** Representative images of DAPI+ cells (blue) and Chr2-EYFP+ cells (green) in the

DG (**C**) and BLA (**D**). % freezing levels throughout optogenetic stimulation of cells active in DG (**E**) and BLA (**I**): 2-Way ANOVA, Holm-Sidak's multiple comparisons: for FC'd DG first light-on vs light-off t=3.821, *p=0.0385. % freezing levels for the light-off and the averaged light-on sessions in DG (**G**) and BLA (**K**): 2-Way ANOVA, Holm-Sidak's multiple comparisons: for FC'd DG light-on vs light-off t=4.072, **p=0.0018. % self-grooming levels throughout optogenetic stimulation in DG (**F**) and BLA (**J**): 2-Way ANOVA, Holm-Sidak's multiple comparisons: for FC'd DG for light-off vs baseline t=2.897, *p=0.0211; vs first light-on t=3.330, **p=0.0091; vs second light-on t=2.09, *p=0.0153. % self-grooming levels for the light-off and the averaged light-on sessions in DG (**H**) and BLA (**I**): 2-WAY ANOVA, Holm-Sidak's multiple comparisons: for FC'd DG for light-on vs light-off t=3.5578, **p=0.006. Data shows as mean, in E, F, I, J +/- SEM. Detailed statistics shown in Supplemental Text. See also **Fig S3**.

References and Notes:

1. Williamson, J.A., and Austin Williamson, J. Social support, mood, and relationship satisfaction at the trait and social levels.

2. Reavis, R.D., Donohue, L.J., and Upchurch, M.C. (2015). Friendship, Negative Peer Experiences, and Daily Positive and Negative Mood. Social Development *24*, 833–851.

3. Neumann, R., and Strack, F. (2000). "Mood contagion": The automatic transfer of mood between persons. Journal of Personality and Social Psychology *79*, 211–223.

4. Caplin, A., Leahy, J., and Matějka, F. (2015). Social Learning and Selective Attention.

5. Heimer-McGinn, V.R., Wise, T.B., Hemmer, B.M., Dayaw, J.N.T., and Templer, V.L. (2020). Social housing enhances acquisition of task set independently of environmental enrichment: A longitudinal study in the Barnes maze. Learn. Behav.

6. Doulames, V., Lee, S., and Shea, T.B. (2014). Environmental enrichment and social interaction improve cognitive function and decrease reactive oxidative species in normal adult mice. Int. J. Neurosci. *124*, 369–376.

7. Dause, T.J., and Kirby, E.D. (2019). Aging gracefully: social engagement joins exercise and enrichment as a key lifestyle factor in resistance to age-related cognitive decline. Neural Regeneration Res. *14*, 39–42.

8. Kuhlmann, S., Piel, M., and Wolf, O.T. (2005). Impaired memory retrieval after psychosocial stress in healthy young men. J. Neurosci. *25*, 2977–2982.

9. Peleh, T., Eltokhi, A., and Pitzer, C. (2019). Longitudinal analysis of ultrasonic vocalizations in mice from infancy to adolescence: Insights into the vocal repertoire of three wild-type strains in two different social contexts. PLoS One *14*, e0220238.

10. Castellucci, G.A., Calbick, D., and McCormick, D. (2018). The temporal organization of mouse ultrasonic vocalizations. PLoS One *13*, e0199929.

11. Wöhr, M., Seffer, D., and Schwarting, R.K.W. (2016). Studying Socio-Affective Communication in Rats through Playback of Ultrasonic Vocalizations. Current Protocols in Neuroscience, 8.35.1–8.35.17.

12. Simola, N., and Brudzynski, S.M. (2018). Repertoire and Biological Function of Ultrasonic Vocalizations in Adolescent and Adult Rats. Handbook of Ultrasonic Vocalization - A Window into the Emotional Brain, 177–186.

13. Biasi, E., Silvotti, L., and Tirindelli, R. (2001). Pheromone detection in rodents. Neuroreport *12*, A81–A84.

14. Bredy, T.W., and Barad, M. (2009). Social modulation of associative fear learning by pheromone communication. Learn. Mem. *16*, 12–18.

15. Ebbesen, C.L., Bobrov, E., Rao, R.P., and Brecht, M. (2019). Highly structured, partner-sex- and subject-sex-dependent cortical responses during social facial touch. Nat. Commun. *10*, 4634.

16. Hertenstein, M.J. The Communicative Functions of Touch in Humans, Nonhuman Primates, and Rats: A Review and Synthesis of the Empirical Research.

17. Liu, N., Wang, Y., An, A.Y., Banker, C., Qian, Y.-H., and O'Donnell, J.M. (2020). Single housing-induced effects on cognitive impairment and depression-like behavior in male and female mice involve neuroplasticity-related signaling. Eur. J. Neurosci. *52*, 2694–2704.

18. Montagrin, A., Saiote, C., and Schiller, D. (2018). The social hippocampus. Hippocampus *28*, 672–679.

19. Gothard, K.M. (2020). Multidimensional processing in the amygdala. Nat. Rev. Neurosci. *21*, 565–575.

20. Davis, P., and Reijmers, L.G. (2018). The dynamic nature of fear engrams in the basolateral amygdala. Brain Res. Bull. *141*, 44–49.

21. Janak, P.H., and Tye, K.M. (2015). From circuits to behaviour in the amygdala. Nature *517*, 284–292.

22. Duvarci, S., and Pare, D. (2014). Amygdala microcircuits controlling learned fear. Neuron *82*, 966–980.

23. Sun, X., Bernstein, M.J., Meng, M., Rao, S., Sørensen, A.T., Yao, L., Zhang, X., Anikeeva, P.O., and Lin, Y. (2020). Functionally Distinct Neuronal Ensembles within the Memory Engram. Cell *181*, 410–423.e17.

24. Josselyn, S.A., and Tonegawa, S. (2020). Memory engrams: Recalling the past and imagining the future. Science *367*.

25. Felix-Ortiz, A.C., and Tye, K.M. (2014). Amygdala inputs to the ventral hippocampus bidirectionally modulate social behavior. J. Neurosci. *34*, 586–595.

26. Defensor, E.B., Corley, M.J., Blanchard, R.J., and Caroline Blanchard, D. (2012). Facial expressions of mice in aggressive and fearful contexts. Physiology & Behavior *107*, 680–685.

27. Clark, J.W., Drummond, S.P.A., Hoyer, D., and Jacobson, L.H. (2019). Sex differences in mouse models of fear inhibition: Fear extinction, safety learning, and fear–safety discrimination. British Journal of Pharmacology *176*, 4149–4158.

28. Haaker, J., Diaz-Mataix, L., Guillazo-Blanch, G., Stark, S.A., Kern, L., LeDoux, J.E., and Olsson, A. (2021). Observation of others' threat reactions recovers memories previously shaped by firsthand experiences. Proceedings of the National Academy of Sciences *118*, e2101290118.

29. Hennessy, M.B., Kaiser, S., and Sachser, N. (2009). Social buffering of the stress response: diversity, mechanisms, and functions. Front. Neuroendocrinol. *30*, 470–482.

30. Donaldson, Z., Hen, R., Gutzeit, V., Santos, T.L., Sadsad, M., and Denny, C.A. (2016). 25.2 SOCIAL BUFFERING OF CONDITIONED AND INNATE FEAR RESPONSES. Journal of the American Academy of Child & Adolescent Psychiatry *55*, S297.

31. Forcato, C., Burgos, V.L., Argibay, P.F., Molina, V.A., Pedreira, M.E., and Maldonado, H. (2007). Reconsolidation of declarative memory in humans. Learning & Memory *14*, 295–303.

32. Chan, J.C.K., and LaPaglia, J.A. (2013). Impairing existing declarative memory in humans by disrupting reconsolidation. Proc. Natl. Acad. Sci. U. S. A. *110*, 9309–9313.

33. Gisquet-Verrier, P., and Riccio, D.C. (2018). Memory integration: An alternative to the consolidation/reconsolidation hypothesis. Progress in Neurobiology *171*, 15–31.

34. Stefanini, F., Kushnir, L., Jimenez, J.C., Jennings, J.H., Woods, N.I., Stuber, G.D., Kheirbek, M.A., Hen, R., and Fusi, S. (2020). A Distributed Neural Code in the Dentate Gyrus and in CA1. Neuron *107*, 703–716.e4.

35. Tanaka, K.Z., Pevzner, A., Hamidi, A.B., Nakazawa, Y., Graham, J., and Wiltgen, B.J. (2014). Cortical Representations Are Reinstated by the Hippocampus during Memory Retrieval. Neuron *84*, 347–354.

36. Chen, B.K., Murawski, N.J., Cincotta, C., McKissick, O., Finkelstein, A., Hamidi, A.B., Merfeld, E., Doucette, E., Grella, S.L., Shpokayte, M., et al. (2019). Artificially Enhancing and Suppressing Hippocampus-Mediated Memories. Curr. Biol. *29*, 1885–1894.e4.

37. Sara, S.J. (2000). Strengthening the shaky trace through retrieval. Nat. Rev. Neurosci. *1*, 212–213.

38. Inda, M.C., Muravieva, E.V., and Alberini, C.M. (2011). Memory retrieval and the passage of time: from reconsolidation and strengthening to extinction. J. Neurosci. *31*, 1635–1643.

39. Kim, J., Kwon, J.-T., Kim, H.-S., Josselyn, S.A., and Han, J.-H. (2014). Memory recall and modifications by activating neurons with elevated CREB. Nat. Neurosci. *17*, 65–72.

40. Ramirez, S., Liu, X., Lin, P.-A., Suh, J., Pignatelli, M., Redondo, R.L., Ryan, T.J., and Tonegawa, S. (2013). Creating a false memory in the hippocampus. Science *341*, 387–391.

41. Redondo, R.L., Kim, J., Arons, A.L., Ramirez, S., Liu, X., and Tonegawa, S. (2014). Bidirectional switch of the valence associated with a hippocampal contextual memory engram. Nature *513*, 426–430.

42. Kalueff, A.V., Stewart, A.M., Song, C., Berridge, K.C., Graybiel, A.M., and Fentress, J.C. (2016). Neurobiology of rodent self-grooming and its value for translational neuroscience. Nat. Rev. Neurosci. *17*, 45–59.

43. Siegmund, A., and Wotjak, C.T. (2007). A mouse model of posttraumatic stress disorder that distinguishes between conditioned and sensitised fear. J. Psychiatr. Res. *41*, 848–860.

44. LaMotte, A.D., Taft, C.T., Weatherill, R.P., and Eckhardt, C.I. (2017). Social skills deficits as a mediator between PTSD symptoms and intimate partner aggression in returning veterans. J. Fam. Psychol. *31*, 105–110.

45. Cisler, J.M., Bush, K., Scott Steele, J., Lenow, J.K., Smitherman, S., and Kilts, C.D. (2015). Brain and behavioral evidence for altered social learning mechanisms among women with assault-related posttraumatic stress disorder. J. Psychiatr. Res. *63*, 75–83.

46. Dutton, C.E., Rojas, S.M., Badour, C.L., Wanklyn, S.G., and Feldner, M.T. (2016). Posttraumatic Stress Disorder and Suicidal Behavior: Indirect Effects of Impaired Social Functioning. Arch. Suicide Res. *20*, 567–579.

47. Cai, D.J., Aharoni, D., Shuman, T., Shobe, J., Biane, J., Song, W., Wei, B., Veshkini, M., La-Vu, M., Lou, J., et al. (2016). A shared neural ensemble links distinct contextual memories encoded close in time. Nature *534*, 115–118.

48. Yetton, B.D., Cai, D.J., Spoormaker, V.I., Silva, A.J., and Mednick, S.C. (2019). Human Memories Can Be Linked by Temporal Proximity. Front. Hum. Neurosci. *13*, 315.

49. Lee, S.-C., Amir, A., Haufler, D., and Pare, D. (2017). Differential Recruitment of Competing Valence-Related Amygdala Networks during Anxiety. Neuron *96*, 81–88.e5.

50. Rodríguez Manzanares, P.A., Isoardi, N.A., Carrer, H.F., and Molina, V.A. (2005). Previous stress facilitates fear memory, attenuates GABAergic inhibition, and increases synaptic plasticity in the rat basolateral amygdala. J. Neurosci. *25*, 8725–8734.

51. Pickens, C.L., Golden, S.A., Adams-Deutsch, T., Nair, S.G., and Shaham, Y. (2009). Long-lasting incubation of conditioned fear in rats. Biol. Psychiatry *65*, 881–886.

52. Campbell, E.J., and Marchant, N.J. (2018). The use of chemogenetics in behavioural neuroscience: receptor variants, targeting approaches and caveats. British Journal of Pharmacology *175*, 994–1003.

53. Grella, S.L., Fortin, A.H., McKissick, O., Leblanc, H., and Ramirez, S. (2020). Odor modulates the temporal dynamics of fear memory consolidation. Learn. Mem. *27*, 150–163.

54. Defensor, E.B., Corley, M.J., Blanchard, R.J., and Blanchard, D.C. (2012). Facial expressions of mice in aggressive and fearful contexts. Physiol. Behav. *107*, 680–685.

55. Jendryka, M., Palchaudhuri, M., Ursu, D., van der Veen, B., Liss, B., Kätzel, D., Nissen, W., and Pekcec, A. (2019). Pharmacokinetic and pharmacodynamic actions of clozapine-N-oxide, clozapine, and compound 21 in DREADD-based chemogenetics in mice. Sci. Rep. *9*, 4522.

56. Liu, X., Ramirez, S., Pang, P.T., Puryear, C.B., Govindarajan, A., Deisseroth, K., and Tonegawa, S. (2012). Optogenetic stimulation of a hippocampal engram activates fear memory recall. Nature *484*, 381–385.

57. Roy, D.S., Park, Y.G., Ogawa, S.K., Cho, J.H., and Choi, H. (2019). Brain-wide mapping of contextual fear memory engram ensembles supports the dispersed engram complex hypothesis. bioRxiv.

58. Pennington, Z.T., Dong, Z., Feng, Y., Vetere, L.M., Page-Harley, L., Shuman, T., and Cai, D.J. (2019). ezTrack: An open-source video analysis pipeline for the investigation of animal behavior. Sci. Rep. *9*, 19979.

59. Ollion, J., Cochennec, J., Loll, F., Escudé, C., and Boudier, T. (2013). TANGO: a generic tool for high-throughput 3D image analysis for studying nuclear organization. Bioinformatics *29*, 1840–1841.

Acknowledgments: Behavioral timelines created with Biorender.com. The authors would like to thank Dr. Susumu Tonegawa and his lab for providing the activity-dependent virus cocktail. **Funding:** This work was supported by an NIH Early Independence Award (DP5 OD023106-01), an NIH Transformative R01 Award, a Young Investigator Grant from the Brain and Behavior Research Foundation, a Ludwig Family Foundation grant, the McKnight Foundation Memory and Cognitive Disorders Award, and the Center for Systems Neuroscience and Neurophotonics Center at Boston University. **Author contributions:** Conceptualization: ABF, HL, RC, YZ and SR; investigation: ABF, HL, RC, TG, AV; methodology: ABF, HL, TG; resources: SR; supervision: ABF, SR; visualization: ABF, HL, RC; formal analysis: ABF and HL; writing - original draft: ABF, RC, HL; writing - review and editing: all authors; and funding acquisition: SR. **Competing interests:** Authors declare no competing interests; and **Data and materials availability:** All data is available in the main text or the supplementary materials.

Supplementary Materials for

Social Reactivation of Fear Engrams Enhances Recall

Abby Basya Finkelstein, Héloïse Leblanc, Rebecca Cole, Troy Gallerani, Anahita Vieira, Yosif Zaki, Steve Ramirez

Correspondence to: afinkelstein@fas.harvard.edu and dvsteve@bu.edu

This PDF file includes:

Materials and Methods
Supplementary Text
Figs. S1 to S3
Captions for Movies S1 to S2

Other Supplementary Materials for this manuscript include the following:

Movies S1 to S2

Materials and Methods

Surgery

465 For all surgeries, mice were initially anesthetized under 3.5% isoflurane inhalation and then maintained during surgery at 1.0-2.0% isoflurane inhalation through stereotaxic nosecone delivery. Ophthalmic ointment was applied to both eyes to provide adequate lubrication and prevent corneal damage. The hair above the surgical site was removed with scissors and subsequently cleaned with alternating applications of betadine solution and 70% ethanol. 2.0% Lidocaine HCl was injected
470 subcutaneously as local analgesia prior to 10-15mm midsagittal incision of the skin. For optogenetic implant surgeries, two bone anchor screws were secured into the cranium, one anterior and one posterior to the target injection and fiber placement sites. All animals then received bilateral craniotomies with a 0.6 mm drill-bit for dorsal dentate gyrus (dDG) and basolateral amygdala (BLA) injections. For all dDG and BLA surgeries, a 10µL air-tight Hamilton syringe with attached 33-gage beveled needle was
475 lowered to the coordinates for DG of -2.2mm anteroposterior (AP), ±1.3mm mediolateral (ML), -2.0mm dorsoventral (DV), and for BLA of -1.35mm (AP), ±3.25mm mediolateral (ML), and -5.0mm (DV). All coordinates are given relative to bregma (mm). For overlap surgeries, a volume of 300 nL of AAV9-cFos-tTa + TRE-EYFP viral cocktail was bilaterally injected at 200 nL/min using a micro-infusion pump for each coordinate (2x300 nL for dDG and 2x300 nL for BLA) (UMP3; World Precision
480 Instruments). After injection was complete, the needle was left in place 2 minutes prior to incremental retraction of the needle from the brain. For dDG chemogenetic surgeries, a 300nL viral cocktail of AAV9-cFos-tTa + AAV9-TRE-hM4Di was bilaterally injected into the dDG at the coordinates listed above. For dDG **or** BLA optogenetic surgeries, a 300nL viral cocktail of AAV9-cFos-tTa + AAV9-TRE-ChR2-EYFP was bilaterally injected into the dDG **or** BLA (separate surgeries and animals for
485 each brain region; see overlap surgeries for coordinates and procedure for injection). Following viral

injection, bilateral optical fibers (200µm core diameter; Doric Lenses) were placed 0.4mm above the injection sites (dDG: -1.6mm DV; BLA: -4.6mm DV). The implants were secured to the skull with a layer of adhesive cement (C&M Metabond) followed by multiple layers of dental cement (Stoelting). Mice were injected with a 0.1 mg/kg intraperitoneal dose of buprenorphine (volume dependent on weight of animal) and placed in a recovery cage atop a heating pad until recovered from anesthesia. Viral targeting was confirmed by histological study and only animals with proper viral expression were utilized for data analysis.

Immunohistochemistry

Mice were overdosed with 3% isoflurane and perfused transcardially with cold (4°C) phosphate-buffered saline (PBS) followed by 4% paraformaldehyde (PFA) in PBS. Brains were extracted and kept in PFA at 4°C for 24-48 hours and then transferred to PBS solution. Brains were sectioned into 50µm thick coronal sections with a vibratome and collected in cold PBS. Sections were blocked for 1-2 hours at room temperature in PBS combined with 0.2% triton (PBST) and 5% normal goat serum (NGS) on a shaker. Sections were incubated in primary antibody (1:1000 rabbit anti-c-Fos [SySy]; 1:5000 chicken anti-GFP [Invitrogen]) made in PBST-NGS at 4°C for 48 hours. Sections then underwent three washes in PBST for 10 minutes each, followed by a 2 hour incubation period at room temperature with secondary antibody (1:200 Alexa 555 anti-rabbit [Invitrogen]; 1:200 Alexa 488 anti-chicken [Invitrogen]) made in PBST-NGS. Sections then underwent three more wash cycles in PBST. Sections were mounted onto microscope slides (VWR International, LLC). Vectashield HardSet Mounting Medium with DAPI (Vector Laboratories, Inc) was applied and slides were coverslipped and allowed to dry overnight. Once dry, slides were sealed with clear nail polish on each edge and stored in a slide box in the fridge. If not mounted immediately, sections were stored in PBS at 4°C.

Behavior

510 *Fear Conditioning* - Fear conditioning (FC) for all experiments took place in a 18.5 × 18 × 21.5 cm chamber with aluminum side walls and plexiglass front and rear walls (Context A). Each cage animal was placed in a separate chamber (4) and received shocks in parallel during the session. The session consisted of 4 shocks over a time span of 500s (shocks at 198s, 278s, 358s, 438s). Depending on the experiment, the length and strength of the shock varied. For the experiments without extinction training
515 (recall 24hrs after social session), the four shocks were 1 second each at 1mA. For the experiments with extinction, in order to obtain homogenous and reliable fear responses at a more remote time point, more intense fear conditioning was utilized, with shocks at 1.5mA for 2 seconds. After the session, animals were placed back into their home cage and in an isolated holding area until all animals in a cohort had been fear conditioned.

520

Extinction Training - Animals were placed into Context A (see above) for a duration of 30 minutes on the day following fear conditioning. A second extinction training session occurred on the next day (30 minutes). All animals in a cage of four underwent extinction training simultaneously. After the session, animals were placed back into their home cage and in an isolated holding area until all animals in a
525 cohort had undergone extinction training.

Extinction Test - For the extinction test, animals were placed into Context A for a duration of 5 minutes. Depending on the experiment, the five minute extinction test was used to assess successful extinction and occured on the day following the second session of extinction training. As in fear conditioning and
530 extinction training, all animals in a cage of four underwent testing simultaneously and were placed back into their home cage and in an isolated holding area until all animals in a cohort were tested.

Recall Test - For the recall test, animals were placed into Context A for a duration of 5 minutes. As in fear conditioning and extinction training, all animals in a cage of four underwent testing simultaneously and were placed back into their home cage and in an isolated holding area until all animals in a cohort were tested.

Generalization - To assess generalization, 24 hours after the recall session animals were placed into Context B (see above for description) for a duration of 5 minutes. All animals in a cage of four underwent testing simultaneously and were placed back into their home cage and in an isolated holding area until all animals in a cohort were tested.

Juvenile Intruder/Cagemate Control - Animals were removed from the home cage and placed into a separate, clean cage with access to food and water. The lid of the cage and the feeder were removed from the home cage, which served as the interaction chamber. An experimental mouse was placed back into the home cage and allowed 1 minute to acclimate. An unfamiliar younger (p43-49) intruder mouse was placed into the home cage for ten minutes of interaction with the experimental resident mouse; younger mice were used to avoid confounding effects of mutual aggression [31,57]. A clear acrylic top was placed over the home cage during interaction. This was repeated for each experimental cage animal. A different intruder mouse was used in each session. After each session, both mice were removed from the home cage and placed into a separate holding cage for their respective group. For cagemate control experiments, a cagemate of the resident mouse was used for interaction in lieu of the unfamiliar intruder. The social session was conducted with a procedure otherwise identical to that used for RIT.

555 *Immediate Shock* - Immediate shock was administered in a 18.5 × 18 × 21.5 cm chamber with vertical black and white striped (3 cm width) sides, a plastic container holding gauze soaked in almond extract under the chamber floor, and red light as room illumination (Context B). The animal received a single 1.5mA shock if after extinction or 1mA shock if without extinction at the 2 second time point over a 60s session.

560

Full Interaction - The lid of the cage and the feeder were removed for social interaction and a clear acrylic top was placed over the home cage. The recently shocked cagemate was then placed into the cage and all animals were left in the testing room for one hour of social interaction. After one hour, the home cage was returned to its normal condition.

565

1-Way Mirror/Mirror No Mouse Control/Opaque Control - Mirror inserts were created out of laminated cardboard and one way mirror material (OuBay). Wooden dowels were placed on the bottom to support the structure. Dimensions were based to fit tightly into the cage (7" x 11" x 5") to separate the container into two sections (a smaller area for the recently shocked cagemate and larger area for the rest of the
570 cagemates). The lid of the cage and the feeder were removed for social interaction and a clear acrylic top was placed over the home cage. In order to enhance the effect of the mirror by creating a large light difference, black covers were created to cover the section of the cage with the recently shocked cagemate. Refer to **Figure S1** for a visual representation of the set-up. After Immediate Shock, the recently shocked cagemate was immediately placed into the section opposite of and separate from the
575 other cagemates. Animals were left in the testing room for one hour of social interaction except in the chemogenetic inhibition experiment, in which they were weighed and injected 15 minutes prior to Immediate Shock and then left to experience the 1-Way Mirror manipulation for 15 minutes to ensure

efficacy of CNO in brain tissue throughout the entire experience[58]. After one hour, or 15 minutes for the chemogenetic experiment, the recently shocked cagemate was removed and immediately euthanized by overdose with sodium pentobarbital to ensure any subsequent effects were due to the manipulation rather than any social interaction afterward, and the home cage was returned to its normal condition. For the Mirror No Mouse Control, all procedural steps were identical to the one-way mirror experiments, except that there was no shocked cagemate placed on the other side of the mirror. For opaque control experiments, the one way mirror insert was altered through the addition of a black insert on the side of the shocked cagemate so that the wall was bidirectionally blocking visual input from the other side. Social interaction was conducted with a procedure otherwise identical to that used for 1-way mirror experiments.

Restraint/Tube Control - One at a time, animals were removed from the home cage and enclosed in a plastic restraint tube containing holes to permit air flow. The tube was then placed in the center of a clean cage for a duration of two minutes. At the end of the two minutes, the animal was released from the tube into a separate clean cage. For the tube control test, all animals remained in the home cage and a clean restraint tube was placed into the home cage for a duration of two minutes.

Female Exposure- One at a time, animals were removed from the home cage and placed into a separate, clean cage for 10 minutes of interaction with an unfamiliar female conspecific. To lessen the females' stress induced resistance to mating, some of the females' bedding was sprinkled into the cage and the females were habituated to the new environment for 1 minute prior to introduction of the experimental male. A clear acrylic top was placed over the cage during interaction. This was repeated for each experimental cage animal. A different female was used in each session. After each session, both mice

were removed from the interaction cage and placed in a new cage, so that naive animals could not interact with those that had already gone through the experience.

Optogenetic Stimulation

605 The optogenetic stimulation session occurred 24 hours after the tagging experience (1-Way Mirror). Prior to the start of the session, optogenetic patch cords were tested to ensure a minimum 10mA laser output. Mice were given stimulation in a separate room than Context A or B. For stimulation, the mice were attached to the optogenetic cords in the palm of ABF's hand and placed into a striped acrylic chamber with either white or dimmed white + red light and either almond or orange scent (Context C).
610 The session lasted 8 minutes and consisted of 4 alternating 2 minute periods of laser stimulation (off/on/off/on; dDG: 450 nm, 20 Hz, 10 ms pulse width[59]; BLA: 450 nm, 4 Hz and 20 Hz, 10 ms pulse width[60]). The BLA group received 4 Hz and 20 Hz stimulation counterbalanced in different contexts (orange vs almond scent, white vs red light) separated by about 1.5hrs.

Behavior Scoring

615 *FreezeFrame* - Videos of behavioral sessions were obtained using cameras secured to the chamber either above or to the side of the subject. For extinction, extinction test, and recall sessions, FreezeFrame/View (Coulbourn Instruments; Whitehall, PA) was used to score freezing behavior, defined as 1.25 seconds of animal immobility.

620 *ezTrack* - Videos of behavioral sessions were obtained using cameras secured to the chamber either above or to the side of the subject. Videos of the open field test were obtained using a webcam secured above for an aerial view. ezTrack[61] was used to analyze all open field videos. An ROI of the center was defined manually according to the lines present on the floor of the open field arena. The software

tracked the movement of the mouse and calculated the amount of frames in which the mouse moved less than specified parameters (both pixel change and distance traveled). The software then tracked and calculated the amount of frames the mouse spent in the center, which was converted to the amount of time spent in the center according to video parameters.

Manual scoring - For optogenetic sessions, due to cord movement and lighting conditions interfering with automated scoring, all freezing and grooming quantification was done manually. This was then converted to a percentage of time that the mouse spent freezing within the bins of stimulation in the session. Each video was scored for grooming by HL, and for freezing by 2 separate observers (ABF and HL or ABF and RC) whose scores were averaged to mitigate variation in bout length perception. Grooming was defined as any syntactic-chain cephalocaudal grooming, scratching, licking, or other observable forms of non-chain self-grooming performed by the animal[47]. Freezing was defined as any observable complete cessation of movement, other than breathing, by the animal.

Imaging and Cell Counting

All coronal brain slices were imaged through a Zeiss LSM 800 epifluorescence microscope with a 20x/0.8NA objective using the Zen2.3 software. Images of the basolateral amygdala were captured in a 2x2 tile (640x640 microns) Z-stack. Images of the dentate gyrus were captured in a 4x2 tile (1280x640 microns) Z-stack. DAPI and GFP were imaged as separate channels for target verification and ensemble size quantification. For overlap counts, DAPI, cFos, and GFP were imaged (DAPI and cFos simultaneously and GFP as a separate channel). 3-4 different slices were imaged for each animal for averaging.

FIJI Software - Images were processed for greater clarity before quantification. The Subtract Background tool was used to enhance contrast of cells to background, and the Despeckle was used to minimize noise that may interfere with quantification. ROIs were selected using Freehand Selection so that only cells within the brain region would be analyzed. The DAPI channel was segmented using a custom pipeline involving 3D Object Counter. The cFos and GFP channels were initially segmented using a custom pipeline utilizing the 3D Iterative Thresholding tool of 3D ImageSuite [62]. Once cells segmented, the z-stacks were Z-Projected into a single slice image and saved.

Cell Profiler - Segmented images of DAPI, cFos, and GFP were loaded into CellProfiler and run through a pipeline that identified cells with more stringent parameters of size and shape. For overlap quantification, the final step in the pipeline counted all identified objects between the cFos and GFP images that had an overlap of greater than 80%.

Cell Quantification and Analysis - Once cells were counted, the relative amounts of $cFos^+$ only, GFP^+ only, and $cFos^+GFP^+$ (overlap) cells in each slice was normalized over the total amount of DAPI cells present ($cFos^+$/DAPI, GFP^+/DAPI, Overlap/DAPI). Chance of an overlap was defined as ($cFos^+$/DAPI)x (GFP^+/DAPI). Overlap over Chance was then calculated by dividing Overlap/DAPI by the Chance Overlap calculated in the previous step.

Supplementary Text

665 *Statistical Analysis Details*

Figure 2: Socially salient but not directly stressful experience reactivate pre-existing fear ensembles

Fig. 2d: Males, 1-sample t-test: DG Restraint t=0.0667, df=4, p=0.95; Shocked Cagemate t=0.085, df=3, p=0.937. BLA 1-Way Mirror t=2.101, df=7, p=0.0737; Shocked Cagemate t=3.492, df=2, p=0.0731.

Fig. 2e: Females, 1-Way ANOVA: DG $F_{2, 12}$=0.7961, p=0.473. BLA $F_{2,8}$=1.767, p=0.2314.

670 **Fig. 2f**: 1-sample t-test for females, DG Restraint t=1.111, df=6, p=0.3093; 1-Way Mirror t=0.8079, df=4, p=0.4645; Shocked Cagemate t=0.9949, df=2, p=0.4246. BLA Restraint t=1.015, df=3, p=0.385; 1-Way Mirror t=2.302, df=4, p=0.0827; Shocked Cagemate t=7.348, df=1, p=0.0861.

Figure 4: DG ensembles active during social stress drive fear only in previously fear conditioned mice

675 **Fig. 4e**: 2-Way RM ANOVA light x group $F_{6, 57}$=1.628, p=0.1560; light $F_{1.917, 36.43}$=0.9090, p=0.4081; group $F_{62, 19}$=3.959, p=0.0365.

Fig. 4f: 2-Way RM ANOVA light x group $F_{6, 57}$=3.071, p=0.0113; light $F_{3, 57}$=0.3763, p=0.7704; group $F_{2, 19}$=1.645, p=0.2193.

Fig. 4g: 2-Way RM ANOVA light x group $F_{2, 20}$=5.120, p=0.0160; group $F_{2, 20}$=1.801, p=0.1909; light

680 $F_{1, 20}$=5.315, p=0.0320.

Fig. 4h: 2-Way RM ANOVA light x group $F_{2, 19}$=7.889, p=0.0032; group $F_{2, 19}$=2.007, p=0.1619; light $F_{1, 19}$=0.1406, p=0.7118.

Fig. 4i: 2-Way RM ANOVA light x group $F_{6, 36}$=0.3690, p=0.8938; light $F_{3, 36}$=0.1871, p=0.9045; group $F_{2, 12}$=0.7903, p=0.4760.

685 **Fig. 4j**: 2-Way RM ANOVA light x group $F_{6, 36}$=1.266, p=0.2971; light $F_{2.559, 30.71}$=0.6596, p=0.5602; group $F_{2, 12}$=3.119, p=0.0812.

Fig. 4k: 2-Way RM ANOVA light x group $F_{2, 12}$=0.5180, p=0.6084; group $F_{2, 12}$=1.062, p=0.3762; light $F_{1, 12}$=0.8643, p=0.3709.

Fig. 4l: 2-Way RM ANOVA light x group $F_{2, 12}$=2.285, p=0.1443; group $F_{2, 12}$=2.503, p=0.1235; light

690 $F_{1, 12}$=0.2462, p=0.6287.

695

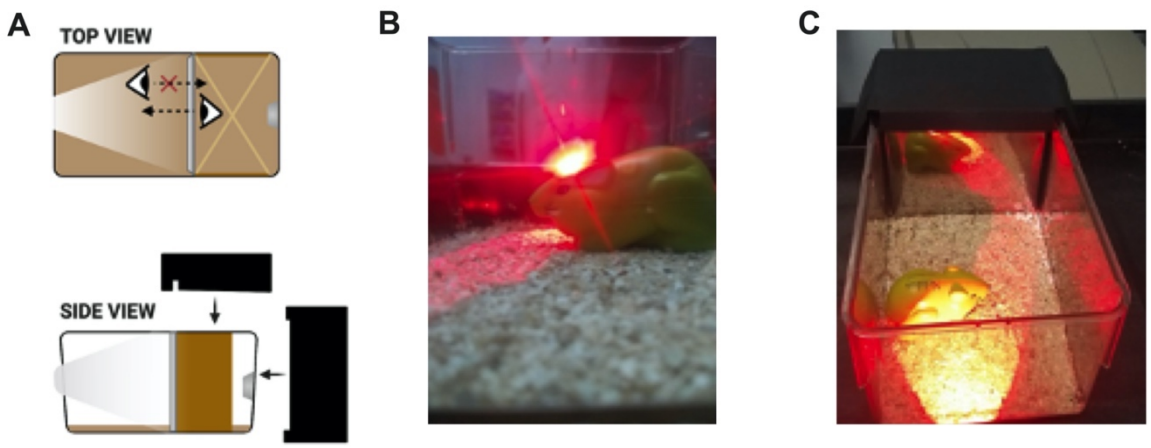

700

Fig. S1. 1-Way Mirror Prototype, Related to Methods. **A)** Unidirectional visual access allows the recently shocked mouse in the darkened compartment to see the cagemates on the other side of the insert, in the bright compartment. **B** and **C)** The cagemates do not see the shocked cagemate in the dark

705 compartment but rather see their own reflections. Auditory-olfactory stimuli are exchanged over the top and sides of the 7” x 11” x 5” insert.

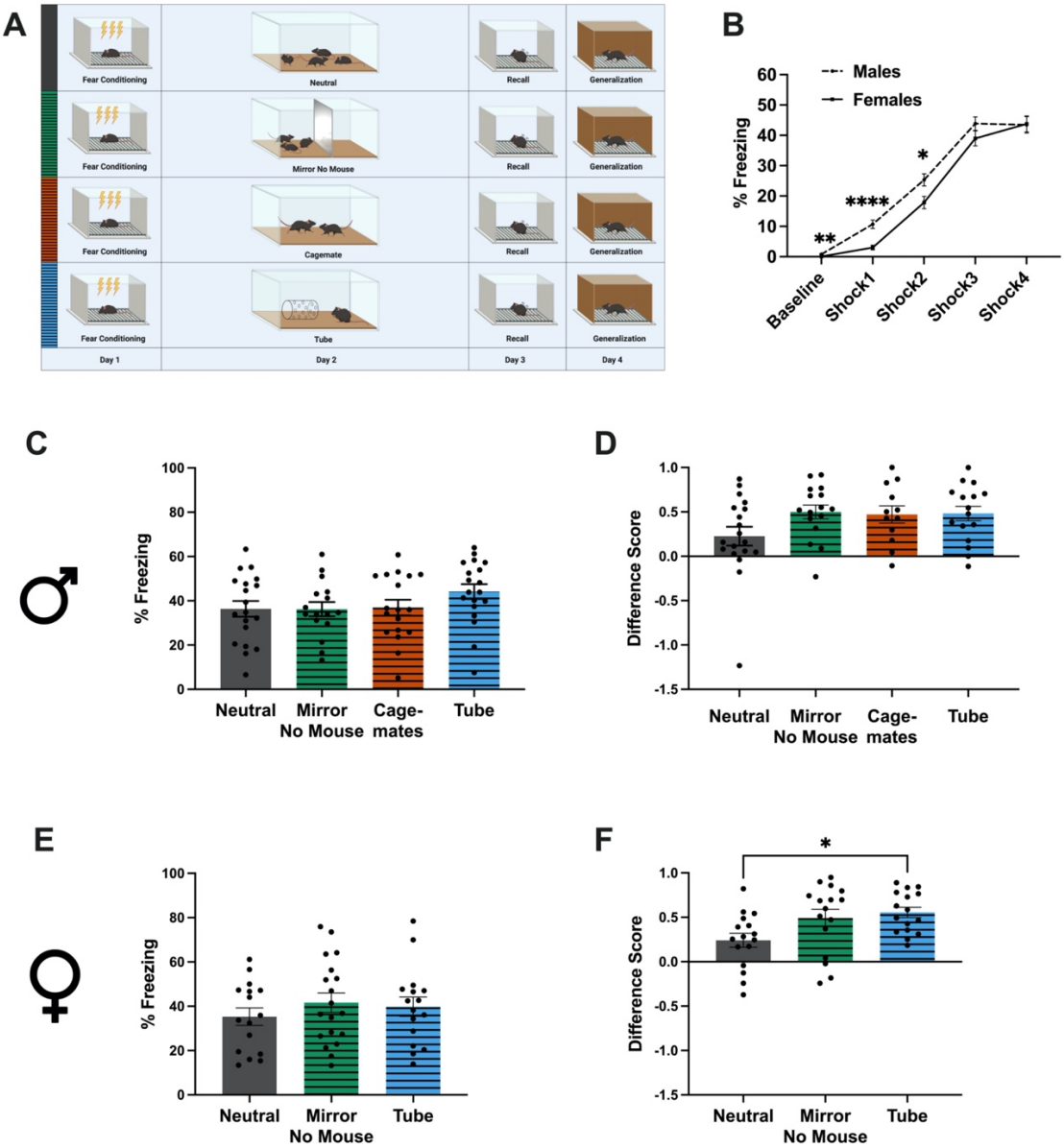

Fig. S2. **Novel objects and neutral social experiences do not impact fear recall. Related to Figure 1.** **A**) Schematic representation of behavioral schedule. **B**) % freezing throughout fear acquisition in males (dashed) and females (solid). 2 Way RM ANOVA with Sidak's multiple comparison tests of fear acquisition for males vs females, n=69 males, n=63 females; Time x Sex $F_{(4, 520)}$=2.910, p=0.0212; Time $F_{(2.717, 353.3)}$=323.8, p<0.0001; Sex $F_{(1, 130)}$=4.895, p=0.0287; Subject $F_{(130, 520)}$=3.594, p<0.0001; Baseline - t=3.336, p=0.0063; Shock1 - t=4.930, p<0.0001; Shock2 - t=2.626, p=0.0475; Shock3 - t=1.464,

p=0.5452; Shock4 -t=0.07762, p>0.9999. **C** and **E**) Freezing levels during a 5 minute fear recall test for

715 males (**C**) and females (**E**). Males: 1-Way ANOVA$F_{(3, 68)}$=1.290, p=0.2848. Females: 1-Way ANOVA$F_{(2, 48)}$=0.5864, p=05603. **D** and **F**) Differences scores, defined as [(freezing in recall test)-(freezing in generalization test)]/(freezing in recall test) for males (**D**) and females (**F**). Males: ANOVA$F_{(3, 59)}$=2.172, p=0.1009. Females: Kruskal-Wallis statistic=8.115, p=0.0173, Dunn's multiple comparisons Tube vs Neutral z=2.551, p=0.0323. Data shown as mean +/- SEM.

720

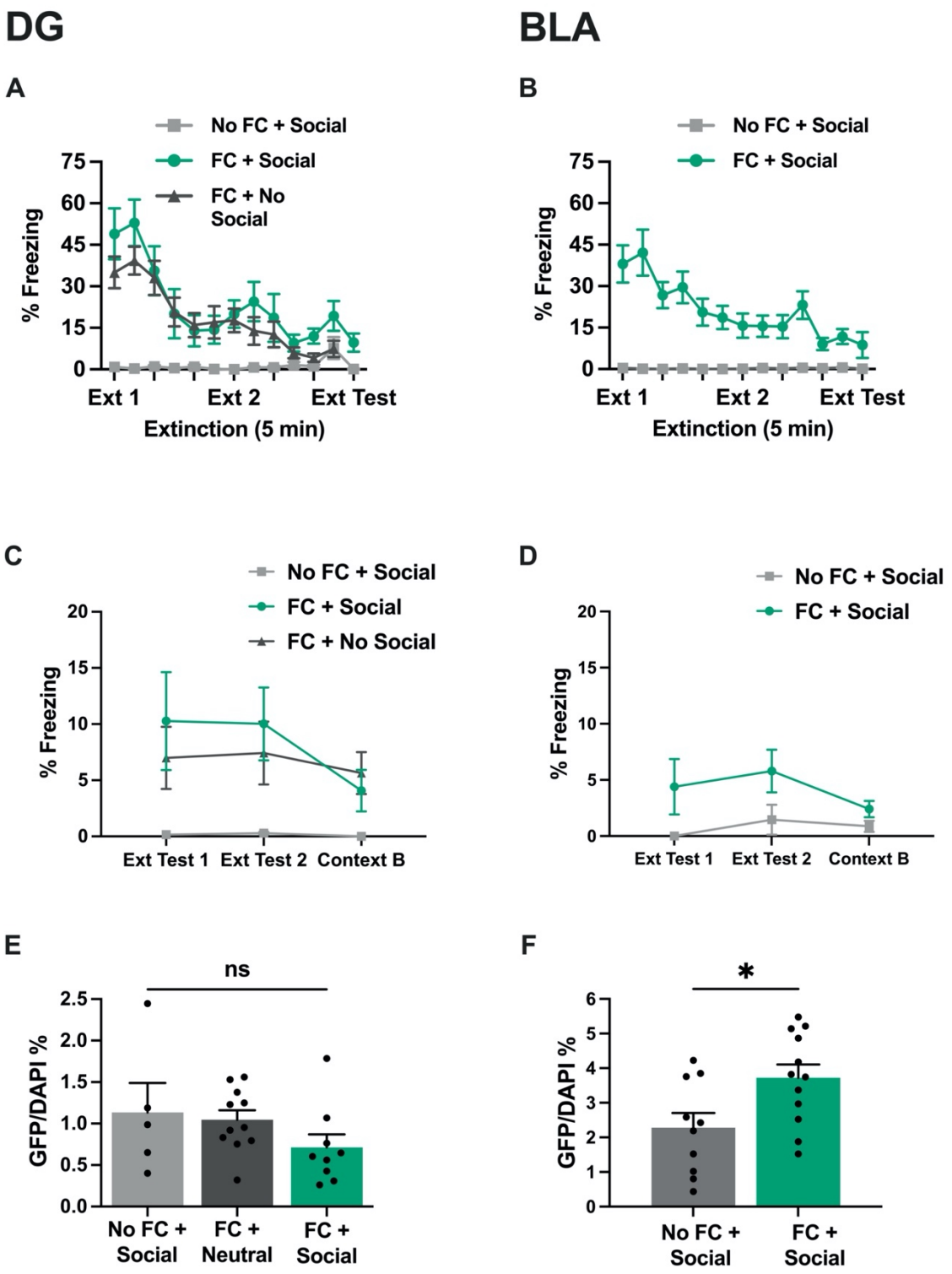

Fig. S3. **Ensemble size and extinction learning curves for optogenetically manipulated groups**. **Related to Figure 4. A** and **B**) % freezing throughout extinction training across groups. Mixed-effects

model (REML), **A**) time p<0.0001, group=0.0025. **B**) time p=0.0016, group <0.0001. **D** and **D**) % freezing during ext test 1, ext test 2 post stimulation, and context b. **E** and **F**) % Chr2-GFP positive cells over total DAPI positive cells. **E**) 1-Way ANOVA $F_{2, 22}$=1.497, p=0.2458. **F**) unpaired 2-tailed t-test t=2.528, df=20, *p=0.02.

Movie S1.

Representative video of 1-way mirror paradigm for fear conditioned cagemates.

Movie S2.

Representative video of juvenile intruder paradigm for fear conditioned cagemates. The experimental resident mouse has two marks at the base of his tail, the intruder has a long solid line from the base to the middle of his tail.